Coupled thermo-hydro-mechanical (THM) processes of high slopes in the Nuozhadu hydropower project on Lancang river in Yunnan province, China

XIAOLI LIU[1], SIJING WANG[2] & ENZHI WANG[3]

[1] *Hydraulics and Engineering Department, Tsinghua University. (e-mail: liuxl04@mails.tsinghua.edu.cn)*
[2] *Institute of Geology and Geophysics of the Chinese Academy of Sciences.*
(e-mail: wangsijing@mail.igcas.ac.cn)
[3] *Hydraulics and Engineering Department, Tsinghua University. (e-mail: nzwang@mail.tsinghua.edu.cn)*

Abstract: The Nuozhadu hydropower project, which is under construction, lies on the Lancang river of Yunnan province in China. This location is in the subtropical zone, with the possible temperature varying from 1.0C to 40.7C, and a mean annual rainfall of 1047.6mm. This project is confronted with many high slopes. In this paper, based on geomechanics and thorough geological investigation, coupled thermo-hydro-mechanical (THM) mathematical models were established to describe the mechanical behaviour of high slopes. These models represent the basic physics of geo-engineering processes, which can include the effects of heat, water and mechanics. The results show that the coupled models are in accordance with the true geological phenomena and more believable. This study is of great academic and engineering significance in analyzing the behaviour of high slopes, and provides a theoretical basis for reasonable selection of countermeasures against slope disasters and for predicting the high slope behaviour after impounding of the reservoir.

Resume: Le projet d'hydro-électricité de Nuozhadu, qui est en construction, se trouve sur le fleuve de Lancang de la province de Yunnan en Chine. Cet endroit est dans la zone subtropicale, avec la température possible changeant de 1.0C à 40.7C, et des précipitations annuelles moyennes de 1047.6mm. ce projet sont confrontées avec beaucoup de pentes élevées. En cet article, basé sur le geomechanics et la recherche géologique complète, (THM) des modèles mathématiques thermo-hydraulique-mécaniques couplés ont été établis pour décrire le comportement mécanique des pentes élevées. Ces modèles représentent la physique de base des processus de geo-technologie, qui peuvent inclure les effets de la chaleur, de l'eau et de la mécanique. Les résultats prouvent que les modèles couplés sont conformes aux véritables phénomènes géologiques et plus crédible. Cette étude est de grande importance d'universitaire et de technologie en analysant le comportement des pentes élevées, et fournit une base théorique pour le choix raisonnable des contre-mesures contre des désastres de pente et pour prévoir le comportement élevé de pente après la confiscation du réservoir.

Keywords: environmental geology, finite element, hydraulic conductivity, permeability, thermal properties, seepage

INTRODUCTION

Among the researches on geo-hazards about engineering rock masses, the single factor which induced directly the geo-hazards was usually studied in detail. For example, when the heat hazards were studied in underground engineering, only the distribution of temperature was solved. When the hazards induced by groundwater seeping were investigated, the fluid seepage pressure was often the main goal. And when the stability of dam foundation was studied in hydropower projects, the distribution of stress in rock masses was focused on. With the development of rock mechanics and engineering practice, the complexity of geological environment which control the engineering rock masses' mechanical properties and the uncertainty of induced geo-hazards were recognized gradually, and the interaction, or the coupling of these factors in geological environment dominating the behaviour of rock masses is presented and studied.

There have been many researches about the coupling phenomena in rock engineering at home and abroad, but it is not enough. The following problems exist. (1) In the 1950s, the coupling phenomena were noticed in analysis of earthquake induced by reservoir, and to the 1970s Witherspoon [1] presented the coupling theory and Noorishad [2] developed one of the first programs for flow analysis in rock masses considering the hydro-mechanical coupling. All these studies were about the coupled hydro-mechanical processes of engineering rock masses. (2) Barton [3] began the preliminary discussion about the coupled thermo-hydro-mechanical processes, but it was just for stability of engineering rock masses and groundwater discharge of tunnels in permafrost regions, and still the overall and systematic theoretical system was lacked at present. (3) In middle of the 1990s, the studies on coupling processes achieved a lot in the research on nuclear waste storage. Jing [4] presented systemic mathematical models of coupled thermo-hydro-mechanical processes, and many more accurate models were developed in DECOVALEX (DEvelopment of COupled models and their VALidation against EXperiments in nuclear waste isolation), an international co-operative research project on mathematical models of coupled THM processes for safety analysis of radioactive waste repositories. But the models are not well suitable widely for application in analysis of hydropower project due to its complexity and not practicality. (4) In China, from the end of the 1980s, many meaningful exploration and studies have been carried on. These researches are mainly about hydro-mechanical coupling or thermo-mechanical coupling, while studies on thermo-hydro-mechanical coupling are few, and especially in engineering of hydropower project, the analysis of coupled THM processes is almost none.

The objective of this paper is to present a simplified thermo-hydro-mechanical coupling model for numerical analyses in hydropower project engineering. By this THM model, the impact of Nuozhadu reservoir impounding and temperature changing to the deformation development of high slopes is analyzed.

GEOLOGICAL BACKGROUND

Nuozhadu hydropower station is located in the lower reach of the Lancang River, in Yunnan province, P.R. China. It is a multi-purpose project with comprehensive benefits in power generation, flood prevention, water supply as well as navigation. The project mainly consists of a core rockfill dam with a maximum dam height of 261.5m, which will be the fourth among the core rockfill dams in the world, and a crest length of 608.16m, and an underground powerhouse with a designed installed capacity of 5850 MW. The reservoir has a normal pool level of 812m and the dead storage level of 765m, and the river's natural water level is around 600m.

Nuozhadu dam site is located in a dissymmetric "V" shaped transverse valley with a slope angle of 40° and 9° above El.1000m on the right bank and 45° below El. 850m on the left bank, and a planation platform exists at El. 850m on the left bank, with a length of 700m along the river and 250m in the mountain. Upstream of the platform is Canjie river and downstream of the platform is Nuozha ravine.

The main strata outcropping in this area consist of Permian Period~Triassic Period Late Variscan-Indosinian granite (γ_4^3~γ_5^1) and granite porphyry (γ_π) intruded later, and Triassic Period siltstones and mudstones ($T_{2m}^{\ 1}$) on the left bank. Moreover, the rock body has been more faulted, excluding the regional fault (class- Ⅰ discontinuity), there are 4 class-II discontinuities, including F_1, F_2, F_3 and F_{35}, 41 class-III discontinuities and 723 class-IV discontinuities. The major faults controlling the slope deformation and stability include faults F_1, F_2, F_3 and F_{35}. The weathered conditions at the dam site are controlled by the topography, rock properties and tectonic action. The weathered depths of rock masses are large and not uniform. The depth of completely and intensely weathered rock masses is not more than 15m below the El. 650m, 20m~60m between the El. 650m~750m, and 40m~100m above the El. 750m. Local unloading is very intense above the El. 680m, the affected depth can be up to 70m, and it is 15m~40m below the El. 680m.

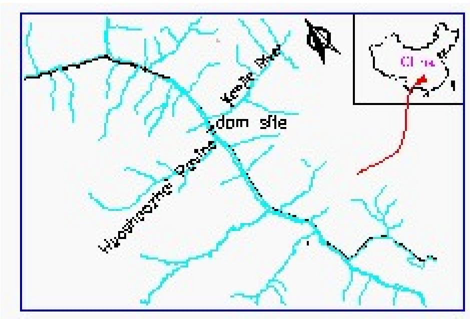

Figure 1. Regional map of Nuozhadu power station site.

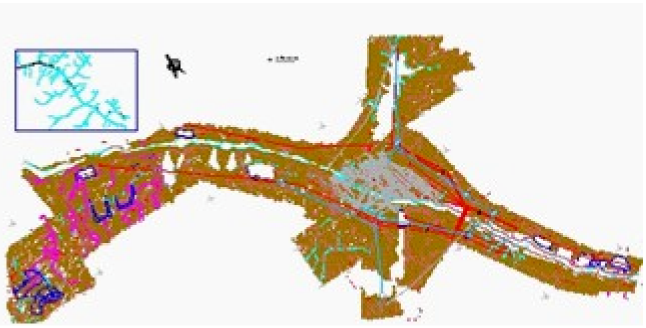

Figure 2. Landform of Nuozhadu dam site.

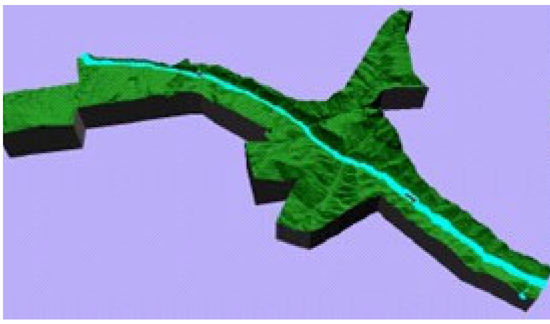

Figure 3. Dam site and before reservoir impounding.

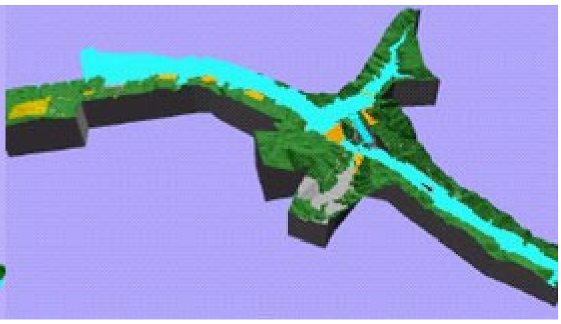

Figure 4. Dam site after reservoir impounding.

MODEL FOR THM COUPLING ANALYSIS

This section proceeds as follows: Firstly it gives the fluid seepage equations, including Darcy's law, continuous equations, state equation and the differential equation of fluid seeping in coupled system. It then describes the coupled THM constitutive relationship, and then gives the equations describing energy transport or energy conservation in coupled system.

Liquid seepage equations

Darcy's law

It is assumed that the liquid flow relating to rock obeys Darcy's law. Suppose $\vec{v}_l$ is the real velocity of the liquid, $\vec{v}_s$ is the real velocity of the solid, and $\vec{v}_r$ is the velocity of the liquid relative to the solid, then the Darcy's law is expressed as follows:

$$\phi\vec{v}_r = -\frac{\vec{K}}{\mu_l}\cdot(\nabla p + \rho_l g \cdot \nabla z) \tag{1}$$

where ρ_l, μ_l represent the density and the viscosity of liquid respectively, and ϕ represents the porosity of the solid (porous media). $\vec{K}$ is the permeability tensor, and $\bar{p}$ is the liquid pressure. $\nabla z = (0,0,1)$ and

$$\vec{v}_r = \vec{v}_l - \vec{v}_s \tag{2}$$

Continuous equations

(1) CONTINUOUS EQUATION FOR LIQUID IN COUPLED SYSTEM

For liquid, the continuous equation is described as following:

$$\frac{\partial(\rho_l\phi)}{\partial t} + \nabla\cdot(\rho_l\phi\vec{v}_l) = 0 \tag{3}$$

Introducing equation (2) to equation (3), and ignoring the second order small quantities $\vec{v}_s\cdot\nabla$ derives the following equation:

$$\rho_l\frac{\partial\phi}{\partial t} + \phi\frac{\partial\rho_l}{\partial t} + \nabla\cdot(\rho_l\phi\vec{v}_r) + \rho_l\phi\nabla\cdot\vec{v}_s = 0 \tag{4}$$

(2) CONTINUOUS EQUATION FOR SOLID

Similarly with the liquid, the continuous equation for solid is written as:

$$\frac{\partial[(1-\phi)\rho_s]}{\partial t} + \nabla\cdot((1-\phi)\rho_s\vec{v}_s) = 0 \tag{5}$$

Expanding Eq. (5) and ignoring the second order small quantities $\vec{v}_s\cdot\nabla$, by multiplying to the every term at left by $\frac{\rho_l}{\rho_s}$ in Eq. (5), we obtain:

$$\frac{(1-\phi)\rho_l}{\rho_s}\frac{\partial\rho_s}{\partial t} - \rho_l\frac{\partial\phi}{\partial t} + (1-\phi)\rho_l\nabla\cdot\vec{v}_s = 0 \tag{6}$$

In Eq. (6), the term $\nabla\cdot\vec{v}_s$ may be written as:

$$\nabla\cdot\vec{v}_s = \frac{\partial}{\partial t}(\nabla\cdot\vec{u}_s) = \frac{\partial}{\partial t}(\delta_{ij}\varepsilon_{ij}) = \frac{\partial\varepsilon_v}{\partial t} = \frac{\partial}{\partial t}(u_{i,i}) \tag{7}$$

where $\vec{u}_s$ represents the displacement vector of the solid particles, $\varepsilon_v = \varepsilon_x + \varepsilon_y + \varepsilon_z = u_{i,i}$, represents volume strain of solid skeleton, and δ_{ij} is Kronecker delta function.

(3) CONTINUOUS EQUATION FOR THE WHOLE SYSTEM

Combining Eq. (4) and Eq. (6), and using Eq. (7), we obtain the continuous equation of the whole system:

$$\phi\frac{\partial\rho_l}{\partial t} + \rho_l\frac{\partial\varepsilon_v}{\partial t} + \frac{(1-\phi)\rho_l}{\rho_s}\frac{\partial\rho_s}{\partial t} + \nabla\cdot(\rho_l\phi\vec{v}_r) = 0 \tag{8}$$

Equations of state

The variables, including density of the liquid and solid ρ_l, ρ_s, viscosity of liquid μ_l, porosity of solid ϕ and permeability tensor, may be expressed as functions of p and T, the state variables denoting the liquid pressure and temperature.

(1) DENSITY AND SOLID POROSITY

With the assumption of small deformation, ρ_l, ρ_s and ϕ are expressed as follows:

$$\rho_l = \rho_{l0}[1 + c_l(p - p_0) - \beta_l(T - T_0)] = \rho_{l0}(1 + c_l\Delta p - \beta_l\Delta T) \tag{9a}$$

$$\rho_s = \rho_{s0}[1 + \frac{p - p_0}{K_m} - 3\beta_{Tm}(T - T_0) - \frac{tr(\sigma' - \sigma_0')}{3K_m(1-\phi)}] \tag{9b}$$

$$\phi = \phi_0[1 + c_\phi(p - p_0) + \beta_\phi(T - T_0)] = \phi_0(1 + c_\phi\Delta p - \beta_\phi\Delta T) \tag{9c}$$

In Eq. (9b), the second term, third term and fourth term in the square brackets denotes the changes of density induced by the liquid pressure, thermal stress, and the effective stress respectively.

Differentiating the density of solid with respect to time derives

$$\frac{(1-\phi)}{\rho_s}\frac{\partial\rho_s}{\partial t} = -\frac{K_b}{K_m}\frac{\partial\varepsilon_v}{\partial t} + \frac{1}{K_m}[(1-\phi) - \frac{K_b}{K_m})]\frac{\partial p}{\partial t} - 3[(1-\phi)\beta_{Tm} - \frac{K_b}{K_m}\beta_{Tm}]\frac{\partial T}{\partial t} \tag{10}$$

where ρ_{l0}, ρ_{s0} and ϕ_0 is the density of liquid, solid and porosity of solid respectively under the reference pressure p_0 and the reference temperature T_0. c_l, c_ϕ, β_l and β_ϕ denotes the compressibility coefficients and the thermal expansion coefficients of liquid and pores in solid, respectively. And K_m, K_b, β_{Tm} and β_{Tb} represents the volume modules and the linear thermal expansion coefficients of solid matrix and the whole body.

Namely

$$c_l = \frac{1}{\rho_{l0}}[\frac{\partial\rho_l}{\partial p}]_0 \qquad c_\phi = \frac{1}{\phi_0}[\frac{\partial\phi}{\partial p}]_0 \qquad c_t = c_l + c_\phi \tag{11a}$$

$$\beta_l = \frac{1}{\rho_{l0}}[\frac{\partial\rho_l}{\partial t}]_0 \qquad \beta_\phi = \frac{1}{\phi_0}[\frac{\partial\phi}{\partial t}]_0 \qquad \beta_t = \beta_l + \beta_\phi \tag{11b}$$

$$\beta_{Tm} = \frac{1}{3\rho_s}\frac{\partial\rho_s}{\partial t} \qquad \beta_{Tb} = \frac{1}{3V_b}\frac{\partial V_b}{\partial t} \tag{11c}$$

where V_b is the volume of the whole body.

Strictly speaking, ϕ is related to the stress and strain of the solid. In this paper, it is assumed that the effect of strain on ϕ is negligible for it is trivial compared to the effect of p and T under the assumption of small deformation.

(2) VISCOSITY OF LIQUID

Experimental results showed: viscosity of water μ_w changes a little with the varying of pressure, and it can be ignored, while it changes obviously with the changing of temperature. According to Kong[10], the values of water viscosity varying from 1.794mPa·s to 0.284mPa·s when the temperature changing from 0°C to 100°C, and the following polynomial expression may be used to describe it:

$$\mu_w = \sum_{k=1}^{5}(-1)^k a_k T^k \tag{12}$$

(3) PERMEABILITY TENSOR

To homogeneous material, the permeability in coupled THM system is described as:

$$K = K_0(1 - c_\phi\Delta p + \beta_\phi\Delta T)(1 + \frac{2}{3}\varepsilon_v) \tag{13}$$

(4) DIFFERENTIAL EQUATION FOR THE LIQUID SEEPING IN COUPLED SYSTEM

Introducing Eq. (2) and Eq. (10) to Eq. (8), and using the equation of state derives the differential equation for the liquid seeping in coupled system as follows:

$$\alpha\frac{\partial\varepsilon_v}{\partial t} + (\frac{\alpha-\phi}{K_m} + c_l\phi)\frac{\partial p}{\partial t} + [3(1-\alpha)\beta_{Tb} - (1-\phi)\beta_{Tm} - \phi\beta_l]\frac{\partial T}{\partial t} = \nabla\cdot[\frac{K}{\mu_l}(\nabla p + \rho_l g\nabla z)] \tag{14}$$

Constitutive equations for the coupled THM system

The total strain consists of thermal strain, liquid pressure induced strain and stress induced strain.

Thermal strain

With the assumptions of linear thermal expansion and solid being the homogeneous material, when the temperature changes from T_{00} to T, the thermal strain is expressed as:

$$\varepsilon_T = \beta_T (T - T_{00})\bar{I} \tag{15}$$

where β_T represents the thermal expansion coefficient tensor.

Strain induced by the liquid pressure

Changing of the liquid pressure in porous media can induce strain. To the isotropic solid material, the strain is written as:

$$\varepsilon_p = -\frac{1}{3K_m}(p - p_0)\bar{I} \tag{16}$$

Strain in the stress field

According to elastic mechanics theory, the strain in the stress field is expressed as:

$$\varepsilon_s = \frac{1}{2G}\sigma' - \frac{\gamma}{2G(1+\gamma)}(tr\sigma')\bar{I} \tag{17}$$

where G is the shear modulus, and γ is a coefficient.

Total strain in the coupled system

Integrating Eq. (15), Eq. (16) and Eq. (17) derives the total strain as follows:

$$\varepsilon = \frac{1}{2G}\sigma' - \frac{\gamma}{2G(1+\gamma)}(tr\sigma')\bar{I} + \beta_{Tb}(T - T_{00})\bar{I} - \frac{1}{3K_m}(p - p_0)\bar{I} \tag{18}$$

The above equation can be easily written as:

$$\sigma' = 2G\varepsilon + \lambda(tr\varepsilon)\bar{I} + \frac{K_b}{K_m}(p - p_0)\bar{I} - 3\beta_{Tb}K_b(T - T_{00})\bar{I} \tag{19}$$

where λ denotes the lame constant.

According to the effective stress law, $\sigma' = \sigma + p\bar{I}$, and using this equation, the Eq. (19) is written as:

$$\sigma = 2G\varepsilon + \lambda(tr\varepsilon)\bar{I} - \alpha p\bar{I} - 3\beta_{Tb}K_b(T - T_{00})\bar{I} \tag{20}$$

Using the Cauchy equations, $\varepsilon_{ij} = \frac{1}{2}(u_{i,j} + u_{j,i})$, the Eq. (20) is expressed by the index symbols as:

$$\varepsilon_{ij} = G(u_{i,j} + u_{j,i}) + \lambda u_{k,k} - 3K_b\beta_{Tb}(T - T_{00})\delta_{ij} - \alpha p\delta_{i,j} \tag{21}$$

Differentiating the terms at both sides of Eq. (21) with respect to x_j derives

$$G\nabla^2 u_i + (G + \lambda)\varepsilon_{v,i} - 3K_b\beta_{Tb}T_{,j}\delta_{ij} - \alpha p_{,j}\delta_{ij} + f_i = 0 \quad (i = 1,2,3) \tag{22}$$

where $f_x = f_y = 0,\ f_z = -[\phi\rho_l + (1-\phi)\rho_s]g$.

Differentiating the terms at both sides of Eq. (22) with respect to t, and noting Eq.(9) derives the constitutive equations of coupled THM system as follows.

$$G\frac{\partial}{\partial t}(\nabla^2 u_x) + (G + \lambda)\frac{\partial^2 \varepsilon_v}{\partial t \partial x} - 3K_b\beta_{Tb}\frac{\partial^2 T}{\partial t \partial x} - \alpha\frac{\partial^2 p}{\partial t \partial x} = 0 \tag{23a}$$

$$G\frac{\partial}{\partial t}(\nabla^2 u_y) + (G + \lambda)\frac{\partial^2 \varepsilon_v}{\partial t \partial y} - 3K_b\beta_{Tb}\frac{\partial^2 T}{\partial t \partial y} - \alpha\frac{\partial^2 p}{\partial t \partial y} = 0 \tag{23b}$$

$$G\frac{\partial}{\partial t}(\nabla^2 u_z)+(G+\lambda)\frac{\partial^2\varepsilon_v}{\partial t\partial z}-3K_b\beta_{Tb}\frac{\partial^2 T}{\partial t\partial z}-\alpha\frac{\partial^2 p}{\partial t\partial z}-\rho_{s0}(1-\alpha)\frac{\partial\varepsilon_v}{\partial t}-[\rho_{l0}\phi c_l+ \\ \rho_{s0}(\frac{\alpha-\phi}{K_m}-\phi_0 c_\phi)]g\frac{\partial p}{\partial t}-[\rho_{l0}\phi_0\beta_l-\rho_{s0}(3(1-\alpha)\beta_{Tb}-3(1-\phi)\beta_{Tm}-\phi_0\beta_\phi)]g\frac{\partial T}{\partial t}=0 \tag{23c}$$

There are 5 variables including liquid pressure p , temperature T and 3 displacement components.

Energy conservation equations for the coupled THM system

According to the first law of thermodynamics, and based on conservation equations of seepage under the non-isothermal condition, the conservation equations for the coupled THM process, the deformation of solid considered, are expressed as the following.

$$\frac{\partial}{\partial t}[\phi\rho_l e_l+(1-\phi)\rho_s c_{sv}T]+(1-\phi)3\beta_{Tm}K_m T\frac{\partial\varepsilon_v}{\partial t}+\nabla\cdot[\rho_l h_l\phi(v_r+v_s)+(1-\phi)\rho_s h_s v_s T]+\nabla\cdot(k_l\nabla T)=q_{ht} \tag{24}$$

where k_l denotes the coefficient of heat conductivity.

At the left side of the above equation, the first term denotes the change rate of the internal energy in system, the second term denotes the change rate of thermal strain energy, the third term is the thermal convection, and the fourth term is the thermal conduction. The term at the right side of Eq. (24) denotes the thermal source intensity. e and h denotes specific internal energy and enthalpy respectively, and may be described as:

$$e_l=c_{lv}(T-T_0)\,,\ h_l=e_l-\frac{p}{\rho}=c_{lp}(T-T_0) \tag{25a}$$

$$h_s=e_s-\frac{1}{\rho_s}\sigma_{ij}\delta_{ij}=c_\phi(T-T_0) \tag{25b}$$

where c_v and c_p denotes constant-volume specific heat and constant-pressure specific heat respectively.

Expanding the first term at the left side of Eq. (24), and replacing Eq. (2) and Eq. (7) into the third term at the left side of Eq. (24) gives the energy conservation equation of coupled THM system as following

$$[\rho_s c_{sv}(\frac{\alpha-\phi}{K_m}-\phi_0 c_\phi)T]\frac{\partial p}{\partial t}-[\rho_s c_{sv}(\phi\beta_\phi+3(1-\phi)\beta_{Tm}-3\frac{K_b}{K_m}\beta_{Tm})T]\frac{\partial T}{\partial t}+[\rho_s c_{sv}(\frac{K_b}{K_m}T+(1-\phi)3\beta_{Tm}K_m T_{00}) \\ +\phi\rho_l c_{lp}T+(1-\phi)\rho_s c_{sp}T]\frac{\partial\varepsilon_v}{\partial t}-\nabla\cdot[\phi_l c_{lp}T\frac{K}{\mu_l}(\nabla p+\rho_l g\nabla z)]+\nabla\cdot(k_l\nabla T)=q_{ht} \tag{26}$$

Combining Eq. (14), Eq. (23) and Eq. (25) establishing the coupled THM mathematical model.

This model is nonlinear, so it is difficult to obtain its analytical solution except for some especially simplified problems. Numerical methods, including FEM, DEM, difference method, and the meshless method developed in recent years, are often adopted to solve it.

ANALYSIS OF THE COUPLED THM PROCESSES OF HIGH SLOPES IN NUOZHADU HYDROPOWER PROJECT

Based on the coupled THM model described above, this paper analyzes the coupled THM processes of high slopes in Nuozhadu hydropower project by adopting the FEM. The purpose is to find out the effect of temperature changing and fluid seeping on the displacement of the high slopes.

The studied area is 1600m×1600m×900m. The finite element mesh is shown in fig. 5, including 66144 nodes and 60060 elements.

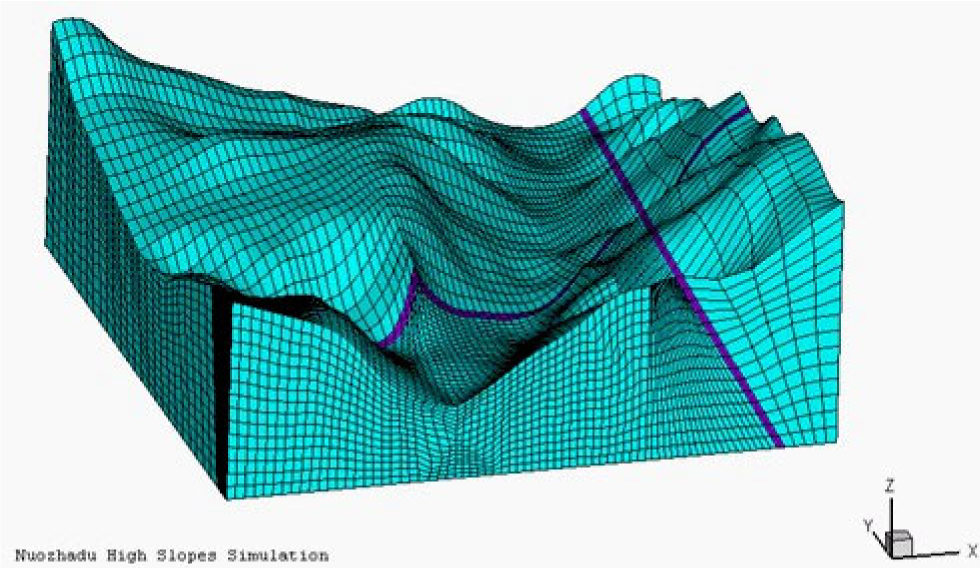

Figure 5. Finite element mesh for the analysis of Nuozhadu high slopes

Boundary and initial conditions and the parameters for THM coupling analysis

For the THM coupling analysis, the boundary and initial conditions should be given in every field respectively.

In temperature field:

$T(x,y,z,t) = 20.9 + 19.9\sin t \quad T(x,y,z,0) = 20.9$ (on the surface of high slopes)

$T(x,y,z,t) = 18$ (on the lower surface)

$F_t(0,y,z,t) = F_t(1600,y,z,t) = 0.05 \quad F_t(x,0,z,t) = 0.025; \quad F_t(x,1600,z,t) = -0.018$

F_t represents the thermal flux.

In seepage field:

$H(x,y,z,t)|_{t=0} = 606 \quad H(x,y,z,t)|_{t>0} = 812$ (on the surface of high slopes)

$F_w(0,y,z,t) = F_w(1600,y,z,t) = 0.068 \quad F_w(x,0,z,t) = 0.045; \quad F_w(x,1600,z,t) = -0.066$

$F_w(x,y,0,t) = 0$

F_w represents the water flux.

In stress field:

The gravity is loaded for every element and the boundary is confined.

$\vec{d}(0,y,z,t) = \vec{d}(1600,y,z,t) = (0,f,f); \quad \vec{d}(x,0,z,t) = \vec{d}(x,1600,z,t) = (f,0,f)$

$\vec{d}(x,y,0,t) = (0,0,0)$

$\vec{d}$ is the displacement vector, and f represent free.

Table.1 parameters of the THM coupling processes for computation

Parameter	value	Parameter	value
Permeability coefficient of rock mass (m/d)	0.0035	Poisson's ratio of rock masses	0.21
Permeability coefficient of faults (m/d)	0.05	Poisson's ratio of faults	0.28
Bulk density of rock masses (N/m^3)	26380	Specific heat (kJ/(kg·°C)) of rock masses	0.9672
Bulk density of faults (N/m^3)	21460	Specific heat (kJ/(kg·°C)) of faults	0.8843
Young's modulus of rock masses (N)	4.1e10	Thermal conduction coefficient of rock masses (kJ/(m·d·°C))	222.48
Young's modulus of faults (N)	1.2e9	Thermal conduction coefficient faults (kJ/(m·d·°C))	198.32

Results of the THM coupling analysis

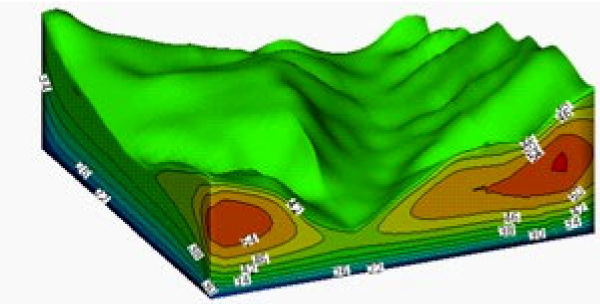

Figure 6. Distribution of the temperature

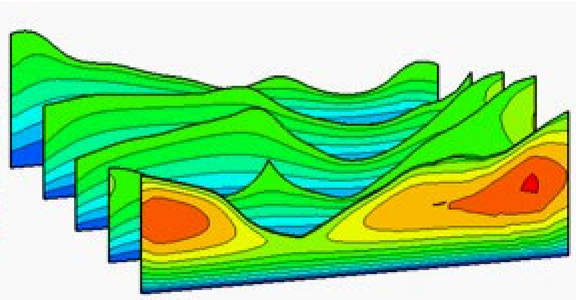

Figure 7. Distribution of the temperature (x direction)

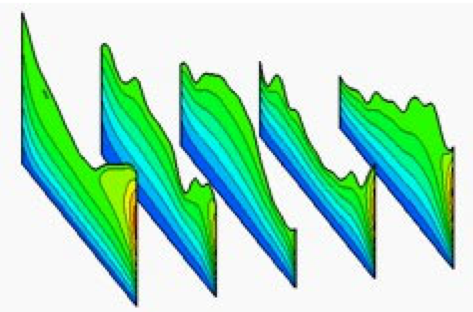

Figure 8. Distribution of the temperature (y direction)

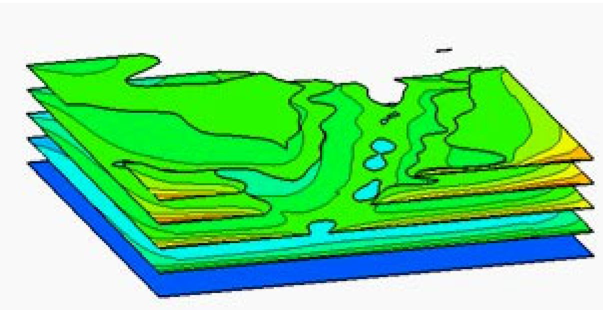

Figure 9. Distribution of the temperature (z direction)

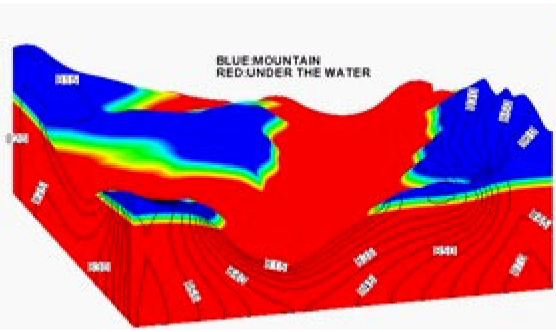

Figure 10. Distribution of the water level in seepage field

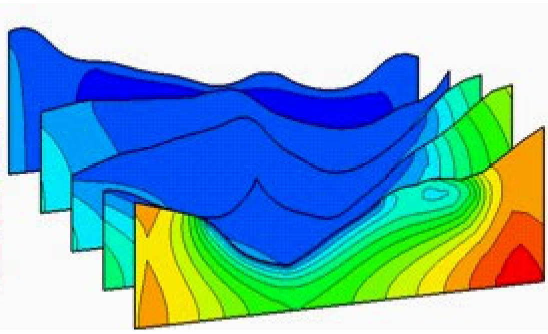

Figure 11. Distribution of the water level in seepage field (x direction)

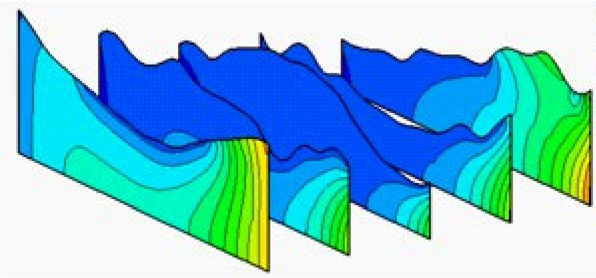

Figure 12. Water level in seepage field (y direction)

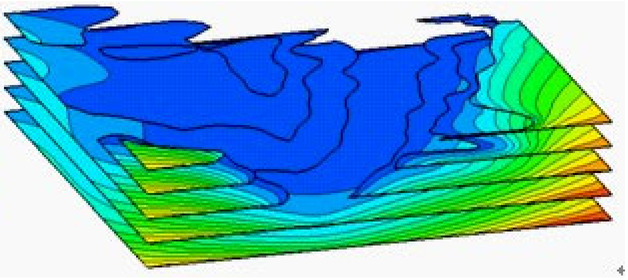

Figure 13. Water level in seepage field (z direction)

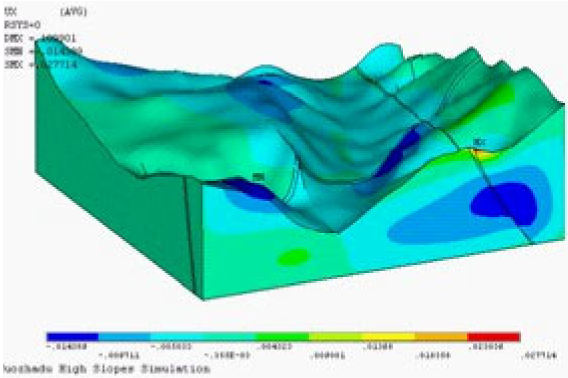

Figure 14. Displacement before reservoir impounding (x direction)

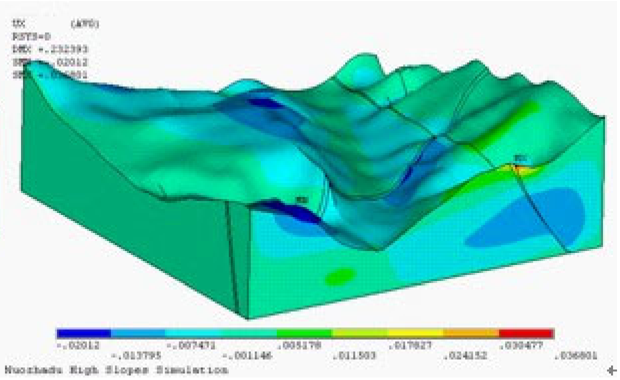

Figure 15. Displacement after reservoir impounding (x direction)

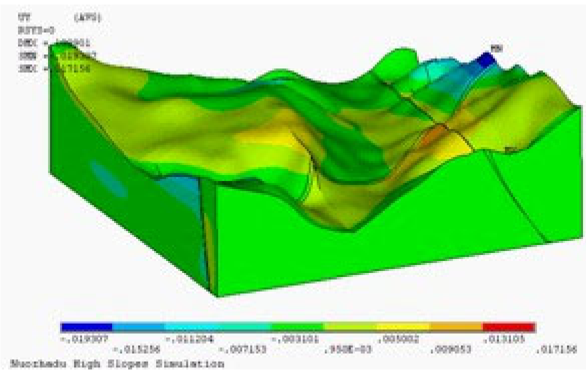

Figure 16. Displacement before reservoir impounding (y direction)

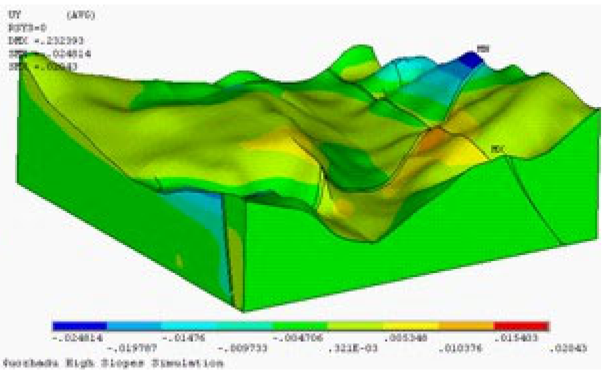

Figure 17. Displacement after reservoir impounding (y direction)

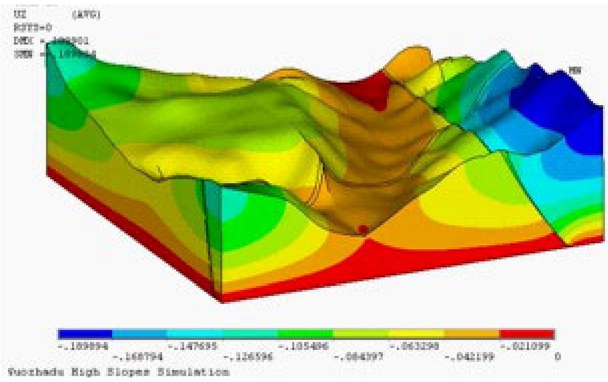

Figure 18. Displacement before reservoir impounding (z direction)

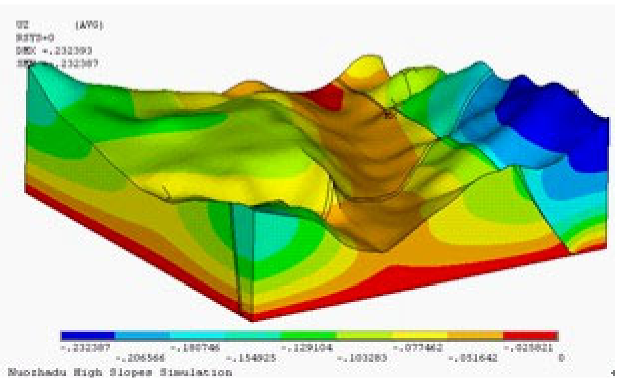

Figure 19. Displacement after reservoir impounding (z direction)

The following figures give the displacement of the high slopes at both sides of the dam site, and they show the differences between the displacements before reservoir impounding and after reservoir impounding by THM coupling analysis.

CONCLUSIONS

The coupled THM phenomena are not emphasized in many fields, especially in design and investigation of hydraulic and hydropower engineering. In this paper, the numerical analyses show that THM processes are very important for the analysis of deformation behaviour of rock masses.

Through systematic study of the THM processes of the high slopes in Nuozhadu dam site, the following conclusions may be reached.

From figure 18, the displacements of the high slopes after the reservoir impounding are almost all negative to x direction. So at the right side of the dam, the high slopes may be move towards the river, which makes the high slopes unstable.

From figure 19, the displacements of the high slopes after the reservoir impounding are not uniform, negative to y direction at left side and positive to y direction at right side. This is notable problem which may make the dam abnormal displacement.

Figure 20 show that, the high slopes show non-uniform subsidence. These places where large displacements happen should be emphasized and studied in detail.

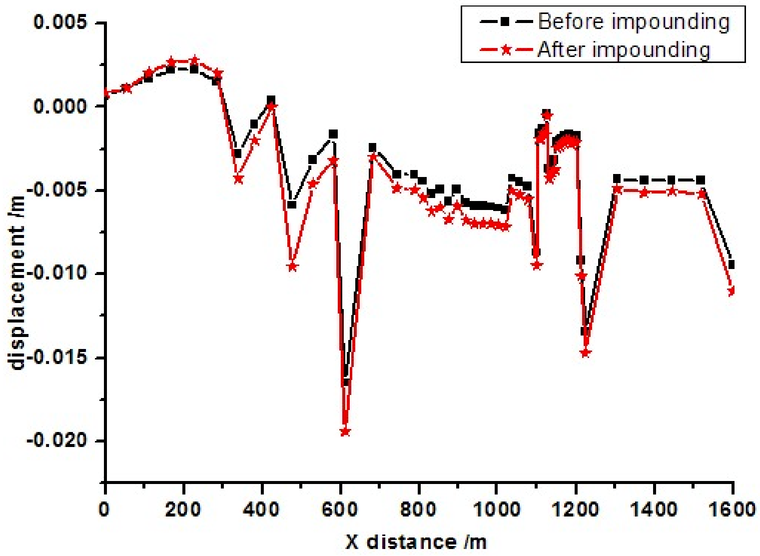

Figure 20. Displacement of the high slopes in x direction at both sides of the dam site

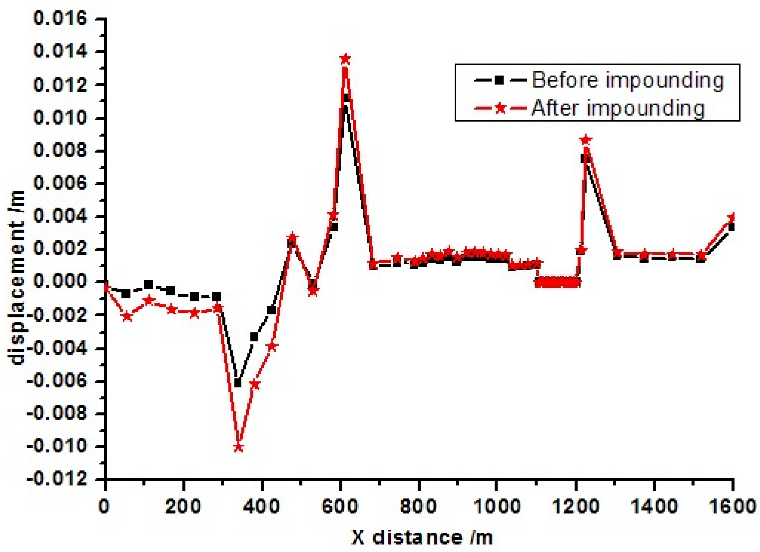

Figure 21. Displacement of the high slopes in y direction at both sides of the dam site

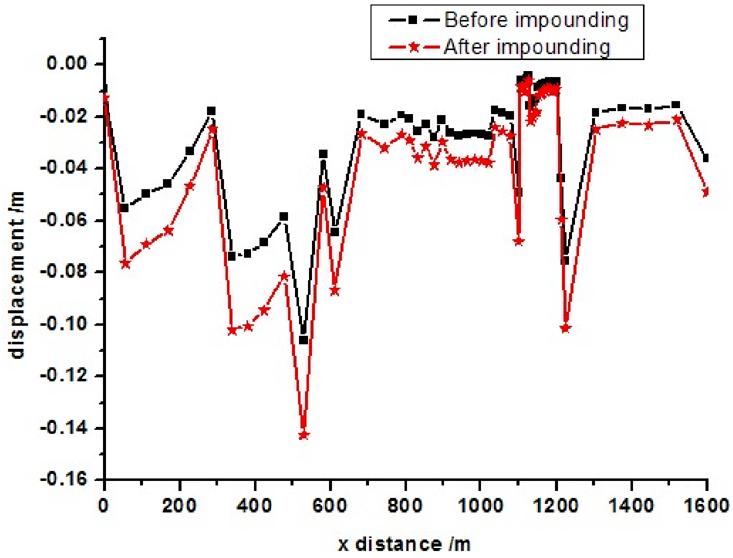

Figure 22. Displacement of the high slopes in z direction at both sides of the dam site

Corresponding author: Mr Xiaoli Liu, Hydraulics and Engineering Department, Tsinghua University, Xueyuan Street of Haidian, Beijing, 100084, China. Tel: +86 10 62794910. Email: liuxl04@mails.tsinghua.edu.cn.

REFERENCES

WITHERSPOON P A, WANG J S Y. 1980. Validity of cubic law for fluid flow in deformable rock fracture. Water Resources Research, 6,112-118

NOORISHAD J, AYATOLLAHI M S. 1982. A finite element method for coupled stress and fluid flow analysis in fractured rock masses. Int. J. Rock Mech. Min. Sci. & Geomech. Abstr. , 19,185-193

BARTON N, BANDIS S C. 1985. Strength, deformation and conductivity coupling of rock joints. Int. J. Rock Mech. Min. Sci. & Geomech. Abstr. , 22(3),121-140

JING L, TSANG C F, STEPHANSSON O.. 1995, DECOVALEX- an international co-operative research project on mathematical models of coupled THM processes for safety analysis of radioactive waste repositories. Int. J. Rock Mech. Min. Sci. & Geomech. Abstr. 32(5),399-408

KONG XIANGYAN, LI DAOLUN, XU XIANZHI, et al. 2005, Study on the mathematical models of coupled thermal-hydrological-mechanical (THM) processes. Journal of Hydrodynamics, 20(2),269-275 (in Chinese)